

Characterization of Quantum Grade Interconnects

R Ferguson¹, S.R.G Hall¹, J Smith¹, R Pitwon², and B Lee³

¹NPL, UK

²Resolute Photonics Ltd, UK

³Senko Ltd, UK

E-mail robert.ferguson@npl.co.uk

Abstract. Quantum grade interconnects, which includes quantum grade optical fibre links and Quantum Photonic Integrated Circuits (QPICs), are rapidly developing components central to the successful development of the Quantum Internet and Quantum Key Distribution (QKD). These interconnects will present new metrological challenges that need to be addressed to ensure key support of future scientific and industrial development. Potential metrological solutions evolving alongside associated standardisation will ensure success and reliability of this advanced technology and provide key support to future scientific research and industrial manufacturing.

1. Introduction

The expectation is that within the next decade, the emerging quantum communication technology market will continue to grow significantly. High levels of investment indicate the confidence that various groups have in the value and economic impact of the rapidly increasing quantum technology market – an assessment found that the market will reach \$31.57 billion within the next four years. [1][2] Significant growth and investment of a strong associated measurement science infrastructure will enable monitoring and quality control of manufacturing processes through traceable metrology. Accurate specifications for industry will support the research and development of new devices.

The National Physical Laboratory (NPL) is well placed to support metrology and standardization of new quantum devices. In particular, advanced interconnects are key enabling components for quantum communications, whether they are local links within hyperscale data centres/exascale computers that incorporate quantum computers and communication nodes, or the long-haul connection of these quantum nodes linked by conventional or specialised fibre-optic networks.

The development of Quantum Key Distribution (QKD) is the first near term application of quantum physics to perfectly secret communication. This requires the transmission of quantum states or qubits to transmit encryption keys to the recipient who can then use conventional communication channels encrypted using these keys. The range of QKD protocols is dependent on the ability of the optical fibre link to preserve the quantum state of the photons. Hence the requirement to characterise optical interconnects to transmit the required quantum states without decoherence is an essential measurement capability which requires development. The longer-term rationale for characterization of quantum grade interconnects is the development of the quantum internet, which will require the transmission of entangled quantum states of photons, to enable distributed quantum computing and superdense coding which can increase channel capacity. Other applications of the quantum internet would include ultra-precise clock synchronisation and improvements to the Global Positioning System (GPS). The generation, deployment and detection of entangled photons will mean that well established ‘classical’ metrology associated with optical fibre is, in many cases, unable to reach the required uncertainties. Yet, there is much that these ‘classical’ platforms can provide by informing methodologies and a

comparative basis to which refinements can be made. High end classical systems such as those at National Measurement Institutes (NMI), can also be used to more fully characterise commercial quantum grade fibre as well as innovative hollow core fibre (HCF) which have up till now, been measured at much lower uncertainties or lack traceability altogether. New bespoke measurement systems will be needed to characterise quantum entanglement efficiencies of discrete Photonic Integrated Circuit (PIC) components.

2. Quantum Grade Connectors and Patchcords

Building upon existing classical characterisation of fibre optics and optical communications research, quantum-grade or quality, optical links and patchcords, can be characterised for existing parameters such as spectral attenuation, insertion loss, return loss, mode field diameter, effective area and numerical aperture. Characterisation of these parameters will be necessary to provide traceable specifications for any commercial company supplying these high quality and novel fibre types. These would encompass deployment of bend insensitive fibre (G657.A1) Hollow Core Fibre (HCF), Photonic Crystal Fibre (PCF) and few-mode fibre. In addition, fibre geometry services have the potential to assess quantum grade connectors and the associated parameters of cladding diameter, non-circularity and core-cladding concentricity of the fibre with respect to the Zirconia ferrule and the mechanical build quality of high-grade connectors.

Fibre connectors are designed to produce a reproducible connection between two fibres, by mechanically aligning the cores of the fibres with each other. The standard metric of connector performance is insertion loss, commonly tested against an "ideal" reference connector. Most connectors are made with a precision drilled hole in a cylindrical ferrule. The stripped and cleaned fibre is inserted into the hole in the ferrule which is filled with epoxy. When the fibre connectors are pushed together, the ferrules are aligned in a sleeve; if the fibre cores lie on their correct respective ferrule axes, aligning the ferrules produces fibre core alignment. Errors in lateral alignment are produced when the fibre cores are eccentric compared with the ferrule axis. This mismatch of cores is considered to be the largest contribution to insertion loss in single-mode connectors. There are connector solutions designed to exhibit the repeatability and low loss required by quantum systems. As an example the E-2000® fibre connector, see figure 1, was originally made by Diamond SA and is claimed to demonstrate a repeatable attenuation at the 0.1db level. This is partially due to the use of ceramic ferrules with titanium inserts instead of the more commonly used ferrule methodology described previously which doesn't use an active crimping alignment process during manufacture, This active process, accurately centres the fibre core on the axis of the ferrule thus ensuring insertion loss is minimized.



E-2000 APC

Figure 1: E-2000 connector Image courtesy of
Senko Inc.

Another connector specifically intended for quantum applications is the Senko QuPC [3] connector has been designed to emulate the specification for a fusion splice i.e. an insertion loss of less than 0.1 dB and an optical return loss less than 60 dB this was achieved by improving manufacturing tolerances of the ferrule hole and controlling the apex of fibre curvature during polishing to coincide with the fibre axis while insuring that fibre undercut or protrusion are managed.

As metrology needs for the Quantum Internet [4] are better understood, the construction of commercially relevant quantum traceable standards becomes essential. This includes the production of bespoke artefacts to calibrate reference Optical Time Domain Reflectors (OTDR's), Optical Frequency domain Reflectometers (OFDR) and Optical Continuous Wave Reflectometer (OCWR's), however, to achieve the dynamic ranges required (>>65dB), investment in state-of-the-art instrumentation and new methodologies is required to achieve meaningful uncertainties.

The pressing need for improved standards for quantum grade optical interconnects was demonstrated by the quotation from the cross-standards (ITU, IEC, IEEE, ETSI, BSI) development forum outputs reported in March 2022 that

“In the short term the most useful standards would be standards for low loss optical interconnect to better allow delicate quantum states, qubits, in the form of single or entangled photons, to be conveyed over longer distances with a lower chance of decoherence and disruption.”

To enable the quantum characterisation of optical interconnects allowing the assessment of entangled photon transmission through connectors, a measurement system using the same principles as the Clauser, Horne, Shimony and Holt (CHSH) [5] experiment can be used to measure the loss of coherence of the entanglement of quantum states through quantum grade links, interconnects or QPICS. By extension, the system can be flexible enough to provide quantum insertion loss measurements (QuIL's) and assessments of quantum coupling efficiencies (QuCE) by incorporating quantum grade interconnects within a test path as well as investigations into link polarization stabilities. The test bed demonstrates evidence of the CHSH inequality, which is a simpler technique than a direct demonstration of Bell's inequalities. In short, it provides experimental confirmation of quantum mechanical behaviour by demonstrating that the degree of correspondence measured cannot be due to classical theory.

The two optical paths (arms) available in the CHSH experimental testbed, shown in figure 2 below, can be used to test components of a quantum communications link by inserting connectors, fibre links or other components into one of the arms of the testbed and then the decoherence of the qubit travelling through that arm can be measured in comparison with the testbed measurements without the insertion of the test artefact.

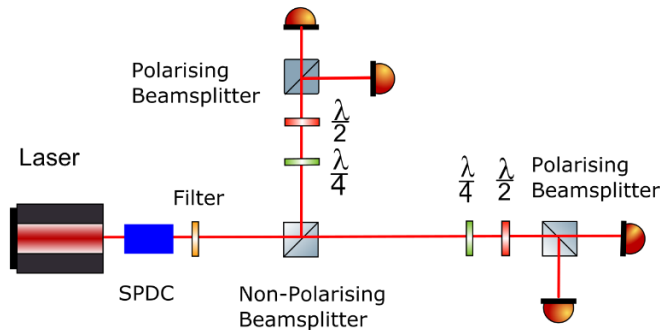


Figure 2: CHSH qubit measurement system

The photon pair used for the system is generated using a periodically poled non-linear KTP (Potassium Dihydrogen Phosphate) crystal using Spontaneous Parametric Down-Conversion (SPDC) where the two photons are produced with frequencies which sum to the frequency of the pump photon. Hence the wavelength of the output photons is half the wavelength of the pump laser photons. The generated photons are orthogonally polarised as this crystal has type II emission. These colinear photons are manipulated with a half wave plate so that one photon was horizontally polarised (H) and one was vertically polarised (V) when they were incident on the beamsplitter, because the two photons have exactly the same properties and only differ in their polarisation state, entanglement is generated at the beam splitter. Each photon has a 50% chance of being transmitted or reflected by the beam splitter. The photons are said to be in a superposition state where we don't know which output port of the beam splitter they have exited until they are measured.

A narrow bandpass wavelength filter allows the removal of photons from the pump laser and fluorescence to be removed before the photons reach a 50/50 beam-splitter that entangles the photons due to their indistinguishability, hence they are produced in a no-deterministic manner. The photons are only post-selectively entangled in that we only know a state has been created subsequent to measurement. The photons can travel down one of two identical arms comprising of half and quarter-waveplates adjusted to a set of angles – and then a second polarising beam-splitter which then further divides the photons into being detected by one of two single-photon detectors (thus there are four detectors in total, two for each arm of the setup - see Fig. 3). A two-photon quantum visibility measurement is a frequently used method of assessing the quality of entanglement using visibility measurements of the vertically and horizontally polarised photons from each arm.

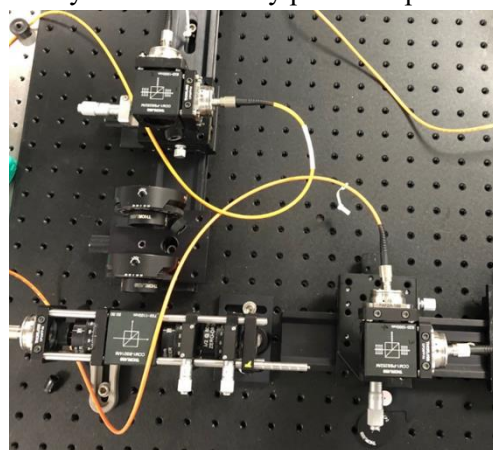


Figure 3: NPL CHSH system. Entangled photons are sent through the system and arrive at one of four single photon detectors, connected to a time tagger that allows for coincidences to be measured.

The CHSH inequality is defined by a parameter "S," where $|S| \leq 2$ and $S = E(\alpha, \beta) - E(\alpha, \beta') + E(\alpha', \beta) + E(\alpha', \beta')$

it should be noted that the negative sign can be moved to any of the other terms in this equation. This results in the effective change of the observable labelling for each qubit.

The terms $E(\alpha, \beta)$ etc. are quantum correlations of particle pairs, these have been defined as the expectation values of the product of the outcomes of the experiment.

Each $E(\alpha, \beta)$ term is given by:

$$E(\alpha, \beta) = \frac{C(\alpha, \beta) - C(\alpha, \beta \perp) - C(\alpha \perp, \beta) + C(\alpha \perp, \beta \perp)}{C(\alpha, \beta) + C(\alpha, \beta \perp) + C(\alpha \perp, \beta) + C(\alpha \perp, \beta \perp)}$$

Where $C(\alpha, \beta)$ is the number of coincidences for the particular values of parameters α and β . In our experimental setup, these values will be the angles of two polarizers, before each polarizing beamsplitter with the outputs incident on Single Photon Avalanche Diodes (SPAD)s.

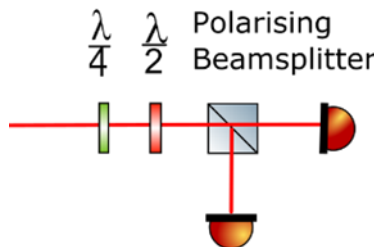


Figure 4.: measurement on one arm with polarisation angle set by the 1/4 and 1/2 waveplate

A coincidence is defined as the simultaneous detection of a photon on both arms. If the coincidences are plotted against the half waveplate angles the resulting sinusoidal fringes demonstrate the violation of the relevant Bell inequality [6]. For the CHSH particular angles $|S| \leq 2$ for any local realistic theory. Hence values of S a significant number of standard deviations above 2 show a violation of Bell's inequality and a demonstration that the testbed is operating in the quantum regime.

Generally, for any single qubit in a pure state (qubits of dimension d where $d=2$) any normalised vector can be described as:

$$|\Psi\rangle = \alpha|0\rangle + \beta|1\rangle [7]$$

Where α and β are complex coefficients and $|\alpha|^2 + |\beta|^2 = 1$

The amplitudes can be interpreted as the probabilities of finding the quantum state $|\psi\rangle$ in the basis state.

Two-qubit polarization states can be represented [8] as:

$$\hat{\rho} = \frac{\begin{matrix} \langle HH| & \langle HV| & \langle VH| & \langle VV| \end{matrix}}{\begin{matrix} |HH\rangle & \begin{pmatrix} A_1 & B_1 e^{i\phi_1} & B_2 e^{i\phi_2} & B_3 e^{i\phi_3} \end{pmatrix} \\ |HV\rangle & \begin{pmatrix} B_1 e^{-i\phi_1} & A_2 & B_4 e^{i\phi_2} & B_5 e^{i\phi_5} \end{pmatrix} \\ |VH\rangle & \begin{pmatrix} B_1 e^{-i\phi_2} & B_1 e^{-i\phi_4} & A_3 & B_6 e^{i\phi_6} \end{pmatrix} \\ |VV\rangle & \begin{pmatrix} B_1 e^{-i\phi_3} & B_1 e^{-i\phi_5} & B_1 e^{-i\phi_6} & A_4 \end{pmatrix} \end{matrix}},$$

Where $\hat{\rho}$ is Hermitian (equal to its own conjugate transpose) and positive with unit trace.

Bell states which have a maximum value of $2\sqrt{2}$ which is Tsirelson's bound (Cirel'son using a different transliteration) [9] are given by:

$$\begin{aligned} |\Psi^+\rangle &= \frac{1}{\sqrt{2}} (|HV\rangle + |VH\rangle), \\ |\Phi^+\rangle &= \frac{1}{\sqrt{2}} (|HH\rangle + |VV\rangle), \\ |\Psi^-\rangle &= \frac{1}{\sqrt{2}} (|HV\rangle - |VH\rangle), \\ |\Phi^-\rangle &= \frac{1}{\sqrt{2}} (|HH\rangle - |VV\rangle), \end{aligned}$$

To obtain the density matrix $\hat{\rho}$ of a mixed state $|0\rangle$ with probability α^2 or $|1\rangle$ with probability β^2 :

$$\hat{\rho} = \sum_m P_m |\Psi_m\rangle \langle \Psi_m|$$

The equation shows $\hat{\rho}$ as an incoherent superposition of pure state density operators $|\Psi_m\rangle \langle \Psi_m|$, where P_m is the probabilistic weighting which incorporates detector efficiency and system losses where $\sum_m P_m = 1$.

As this is a 2^n by 2^n matrix representing the n-qubit state it can be diagonalized.

To be able to change the coincidence rates into probabilities we measure at least one complete basis first and then sum the rates for a complete set of orthonormal projectors to get an approximation of the intensity of incident states. This enables us to derive a probability from any coincidence rate.

This type of tomography is used with a minimum of 9 settings giving 36 measurement results. This system mitigates the laser output drift problem by using pairs of detectors for the measurements thus producing relative intensities rather than absolute measurements.

To summarize we define a probability vector \mathbf{P} which contains the elements of the 36 coincidence counts normalized by sum of the first four measurements (one basis) and an invertible square matrix \mathbf{M} , this is derived from the measurement settings and the Pauli matrices.

So the final vector, given by:

$$\mathbf{M}^{-1} \cdot \mathbf{P},$$

consists of the real and imaginary parts of the density matrix $\hat{\rho}$. The type 1 and type 2 experimental uncertainties [10] inherent in the measurements mean that an algorithm is required which incorporates likely uncertainty values and calculates a state most likely to have generated the experimental results.

Another potential metrological platform is the use of a variable launch system, such as that used at NPL and shown in figure 5 [11,12], that can control the launch of a laser, in terms of spot size and numerical aperture, into a particular waveguide to assess attenuation, encircled flux and bit error ratio. This system provides flexibility to assess individual fibres or waveguides embedded onto interconnect boards as well as silicon-based PIC's/QPIC's and provides information on coupling efficiencies and functional performances under different operating conditions [13]

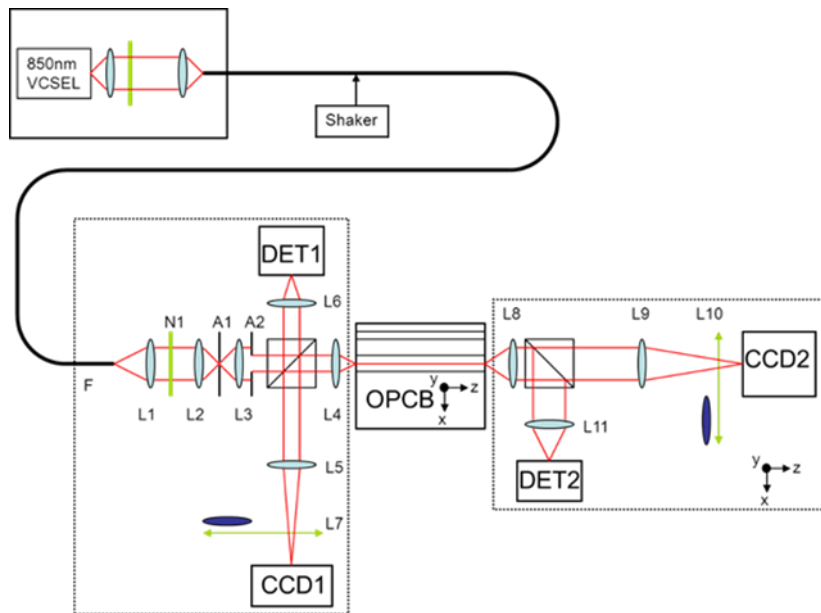


Figure 5:Schematic of NPL Variable Launch System

2 QPIC's

Photonic Integrated Circuits (PICs) have seen extensive development over the past decade and are important components for the future of optical communications and optical metrology (eg: LIDAR and fibre-optic sensing applications).[14,15,16,17]. As well as improving traceable metrology aimed at entire PIC interconnects such as insertion loss, polarization-dependent loss and return loss (including refined single, stepped and swept wavelength measurements), more specific metrology is based around structures and waveguides that perform specific functions. These include optical coupling[18], power splitting, wavelength division multiplexing or active elements affecting optical gain.

[19,20,21]Accessing these structures in order to measure key parameters is technologically challenging and would require ongoing collaboration with manufacturers to develop PIC designs that allow access to key points and probing of test points along waveguide pathways.

Quantum Photonic Integrated Circuits (QPICs or QuPICs) advance PIC technology to the quantum realm and allow for production and/or control of photonic quantum states for quantum applications. They are a compelling platform for extending quantum technologies to wider communication infrastructure - such as allowing for transfer of information in a distributed quantum computing environment. It is envisaged that QPICs will be an enabling technology for any sector where quantum information needs to be transferred or generated remotely, such as quantum encryption, quantum sensing and optical quantum computing. Measuring quantum efficiencies of QPIC's and their respective components using the pathway of a CHSH test platform (See figures 2-4) would provide essential information in order to ensure successful operation at the quantum level.

Fibre tapering, used for fibre to PIC coupling and emerging technologies [22],utilises focused ion beam etching to modify and incorporate features into the end faces of optical fibre altering far-field intensity profiles . These links can be measured effectively by modifying or extending the ranges of existing systems for characterising optical intensity output profiles such as those used for mode field diameter measurements. Aligning optical connections and reducing mode field mismatches is very important in the drive to minimize leakage or losses and is currently a significant challenge to large scale fabrication [23,24,25]. These modified coupling techniques have far-reaching consequences for

improved coupling efficiencies and maximising bandwidth in networks embracing interconnect boards [17,18] as well as PIC's and QPIC's.

3 Longer-haul Quantum Grade links (G657A1/Hollow Core Fibre (HCF))

Bend insensitive fibres such as G657.A1 are already available as quantum grade optical links for patchcords. Commercially available G657.A1 could benefit from more rigorous classical fibre metrology to reduce of the specified uncertainties. For example, a typical MFD value specified on a commercial fibre of this type 8.3 to 9.3 μm at 1550 nm and a dispersion coefficient of ≤ 18 ps/nm/km.[26]. Quantum internet performance will require much more stringent knowledge of these parameters to maximise efficiencies.

Although HCF has been developed over approximately 30 years, only recently has its potential for longer haul communication systems been recognized. With very low losses (< 0.1 dB/km at 1550 nm), low dispersion (3 ps/nm/km) and non-linearities and wide bandwidths, the future deployment for quantum applications is promising once it has become more cost effective to produce in significant lengths.

Several operators around the globe have been deploying HCF in their QKD systems. Following the first industrial deployment of a QKD network in the UK using standard fibre, recent demonstrations have claimed a world first with a trial of QKD over HCF [27] additional security is achieved using a Quantum Random Number Generator (QRNG). It is claimed that the test demonstrated that HCF is an excellent conduit for QKD transmission, enabling reduced latency and cutting down on interference between signals being transmitted over the fibre. This allowed QKD transmission to occur alongside other signals without impacting the security of the key transmission.

4 Conclusions

NPL and other NMI's capability, current expertise and future plans have shown that there is an urgent need to develop systems and traceability [28]. Active involvement is needed in National and International standards bodies to harmonise the global approach towards standards thereby supporting industry and future research and development of this emerging technology. The established expertise of NPL surrounding classical characterisation of optical communication technologies can be used to extend existing or develop new traceable systems. Quantum level metrology will not develop as an autonomous or solely independent technology but will be part of a marriage of classical and bespoke quantum systems that will significantly improve the quality and performance of new and emerging components and build confidence in developers and consumers alike.

Acknowledgements

This project 20SIP05 KTOC has received funding from the EMPIR programme co-financed by the Participating States and from the European Union's Horizon 2020 research and innovation programme, Funder ID: 10.13039/100014132

References

- [1] R and M Ltd, Quantum Technology Market by Computing, Communications, Imaging, Security, Sensing, Modeling and Simulation 2021 - 2026. <https://www.researchandmarkets.com/reports/5317365/quantum-technology-market-by-computing> (accessed Jan. 20, 2022)
- [2] The Vision for the Global Quantum Internet | FifteenEightyFour | Cambridge University Press', Sep. 06, 2021. <https://www.cambridgeblog.org/2021/09/the-vision-for-the-global-quantum-internet/> (accessed Jan. 20, 2022).
- [3] Lee B, Pitwon R Jun 2020 White Paper QuPC® Connectors - Optical Interconnect for Quantum

Networks

[4] Li J, Jia Q, Xue K, Wei DSL and Yu N 2022 A connection-oriented entanglement distribution design in quantum networks, *IEEE Transactions on Quantum Engineering*, **3**, pp. 1-13, , Art no. 4100513, doi: 10.1109/TQE.2022.3176375

[5] Clauser JF, Horne MA, Shimony A, Holt RA 1969 Proposed experiment to test local hidden-variable theories *Phys. Rev. Lett.*, **23** (15): 880–4, Bibcode:1969PhRvL..23..880C, doi:10.1103/PhysRevLett.23.880

[6] Nielsen M, Chuang I 2010 Quantum computation and quantum information: 10th Anniversary Edition. Cambridge: Cambridge University Press. doi:10.1017/CBO9780511976667

[7] Kwiat PG, Mattle K, Weinfurter H, Zeilinger A, Sergienko AV, and Shih Y 1995 New high-intensity source of polarization-entangled photon pairs *Phys. Rev. Lett.* **75**, 4337 –

[8] Altepeter J, James DF, & Kwiat PG 2004 Quantum state tomography chapter in Quantum state estimation DOI: <https://doi.org/10.1007/b98673> eBook ISBN 978-3-540-44481-7

[9] Cirel'son BS 1980 Quantum generalizations of Bell's inequality *Letters in Mathematical Physics*.**4** 2 93–100. Bibcode:1980LMaPh...4...93C. doi:10.1007/bf00417500. ISSN 0377-9017

[10] BIPM, IEC, IFCC, ISO, IUPAC, IUPAP, OIML. Guide to the expression of uncertainty in measurement. international organization for standardization, Geneva. ISBN 92-67- 10188-9, BSI - BS PD 6461-3 General metrology. Part 3: Guide to the expression of uncertainty in measurement (GUM)

[11] Ives D et al, 2011 Development of a variable launch attenuation and isolation measurement system for optical waveguides *Applied Optics* **50** No. 22.

[12] Ferguson R 2012 Waveguides need characterization, too *Photonics Spectra* pp.58-60.

[13] Ferguson RA and Harris S 2007 Development of an optical system with controlled launch conditions for the characterisation of polymer optical fibre (POF)", *Optical Fibre Measurement Conference Digest* **15**

[14] Hogan H, 2017 Senko, 2020 Data centre network: impact on optical interconnect & component technology *Photonics Spectra Lightwave Webcast* p36.

[15] Ingham J D, Bamiedakis N, Penty RV, White IH., DeGroot JV and Clapp TV 2006 Multimode siloxane polymer waveguides for robust high-speed interconnects, *Conference on Lasers and Electro-Optics and 2006 Quantum Electronics and Laser Science Conference*.

[16] Pitwon, R. 2016 Advances in photonic interconnect for data centre subsystems, *Seagate Systems, UK, 4th Symposium on Optical Interconnect in Data Centres*, ECOC 2016, Düsseldorf, Germany.

[17] CIR., 2010. Board-level optical interconnects sales to hit \$5.6 billion by 2022 *Lightwave Staff article*

[18] Selviah D et al 2017 Integrated optical and electronic interconnect PCB manufacturing research, *Circuit World* **36**, 5–19.

[19] IPC-TM-650, 1997. Test Methods Manual, The Institute for Interconnecting and Packaging Electronic Circuits Doc. No. 2.6.7, Rev. A.

[20] IEC 61300-1:2016 - Fibre optic interconnecting devices and passive components – Basic test and measurement procedures – Part 1: General and guidance.

[21] IEC 62496-2:2017 (E) - Optical circuit boards - Basic test and measurement procedures - Part 2: General guidance for definition of measurement conditions for optical characteristics of optical circuit boards.

[22] Marchetti R, Lacava C, Carroll L, Grädowski K, and Minzioni P 2019 Coupling strategies for silicon photonics integrated chips [Invited]," *Photon. Res.* **7**, 201-239

[23] Eisenstein, M 2022 As pic production ramps up, fabricators eye alignment options *Photonics Spectra*

[24] Selviah DR, Fernández FA, Papakonstantinou I, Wang K, Bagshiahi H, Walker AC, Mc-Carthy A, Suyal H, Hutt DA, Conway PP, Chappell J, Zakariyah SS and Milward D, 2008 Integrated optical and electronic interconnect printed circuit board manufacturing *Circuit World*, **34**, pp. 21-26

- [25] Bamiedakis N, Hashim A, Penty RV, White IH, 2012 Regenerative polymeric bus architecture for board-level optical interconnects *Optics Express* **20** 11625 No. 11
- [26] IEC 60793-1-43 Ed. 1.0 (2001-07), Optical fibres - Part 1-43: Measurement methods and test procedures - Numerical aperture, Publication date 26-07-2001
- [27] <https://www.fiercetelecom.com/tech/bt-eyes-quantum-security-boost-hollow-core-fiber-trial>
(accessed Jul. 14, 2022)
- [28] NIST PML Photonics Priority: Metrology for advanced manufacturing
<https://www.nist.gov/pml/pml-priority-photonics/pml-photonics-priority-metrology-advanced-manufacturing>